Journal of Physics: Condensed Matter

Heat capacity study of relaxors $BaTi_{0.65}Zr_{0.35}O_3$ and $BaTi_{0.60}Zr_{0.40}O_3$

To cite this article: Michail Gorev *et al* 2006 *J. Phys.: Condens. Matter* **18** 4407

INSTITUTE OF PHYSICS PUBLISHING JOURNAL OF PHYSICS: CONDENSED MATTER

J. Phys.: Condens. Matter **18** (2006) 4407–4416 doi:10.1088/0953-8984/18/17/026

Heat capacity study of relaxors $BaTi_{0.65}Zr_{0.35}O_3$ and $BaTi_{0.60}Zr_{0.40}O_3$

Michail Gorev[1], Vitaly Bondarev[1], Philippe Sciau[2] and Jean-Michel Savariault[2]

[1] L V Kirensky Institute of Physics, Siberian Division, Russian Academy of Sciences, Akademgorodok, Krasnoyarsk, 660036, Russia
[2] CEMES-CNRS, 31055 Toulouse, France

E-mail: gorev@iph.krasn.ru and sciau@cemes.fr

Received 28 December 2005, in final form 28 March 2006
Published 13 April 2006
Online at stacks.iop.org/JPhysCM/18/4407

Abstract

The heat capacity of two relaxors $BaTi_{1-x}Zr_xO_3$ ($x = 0.35, 0.40$) was measured using adiabatic calorimetry in the temperature range 100–360 K. The $C_p(T)$ dependence of both compositions is characterized by the presence of two diffuse anomalies near the Burns temperature T_d and the temperature of the maximum in permittivity T_m in the temperature ranges 250–350 K and 120–200 K. The anomalous heat capacity near T_d was analysed taking into account the distribution of Zr concentration in nanoregions leading to the distribution of their transition temperatures into the polar phase. Excess heat capacity near T_m was discussed in the framework of the spherical random bond–random field model. The results are compared with the data obtained by the same procedures for $PbMg_{1/3}Nb_{2/3}O_3$ studied experimentally earlier.

1. Introduction

In recent years, the demands for miniaturized circuits and devices have driven the research in microelectronic science and technology for capacitor, memory element and sensing device applications. The lead-based complex perovskites $Pb(Sc_{1/2}Nb_{1/2})O_3$, $Pb(Mg_{1/3}Nb_{2/3})O_3$ and $Pb(Fe_{1/2}Nb_{1/2})O_3$ have attracted much attention for their characteristic dielectric nature, i.e. high dielectric constant and wide temperature stability around the broad diffuse phase transition. However, most such materials contain lead, which pollutes the environment. Therefore, lead-free materials with high dielectric constant are becoming increasingly attractive. Recently, many research works have been reported for ceramic samples of perovskites derived from $BaTiO_3$ by cationic homovalent or heterovalent substitutions [1–5] and exhibited typical relaxor ferroelectric behaviour characterized by a broad and frequency dependent dielectric permittivity maximum at T_m.

The main features of relaxors are connected with their structural (compositional) inhomogeneity or disorder and with the presence of polar nanodomains in nonpolar matrix.

The structural investigations and physical property studies of relaxors reveal three peculiar temperatures: T_d, T_m and T_c. On cooling below T_d small polar nanodomains appear, whose interactions and growth can trigger a transition into a glassy or ordered phase. If the domains become large enough, the sample will undergo a cooperative ferroelectric phase transition at T_c. On the other hand, if the nanodomains grow but do not become large enough, they will ultimately exhibit a dynamic slowing down of their fluctuations below T_m, which is the temperature of the dielectric permittivity maximum, leading to an isotropic relaxor state with random orientation of polar domains [6].

$Ba(Ti_{1-x}Zr_x)O_3$ solid solutions are characterized by both ferroelectric and relaxor properties depending on the composition: the original ferroelectric transitions of $BaTiO_3$ continuously transform into the relaxor state whose temperature of occurrence (T_m) decreases to very low temperatures as the Zr content increases [1–3, 7]. Based on the dielectric response, $BaTi_{1-x}Zr_xO_3$ solid solutions can be classified into three groups [8].

In region I ($x < 0.12$) three dielectric anomalies were observed, which are due to phase transitions from a cubic paraelectric to a tetragonal ferroelectric (at T_c), and then to an orthorhombic ferroelectric (at T_1), and finally to a rhombohedral ferroelectric (at T_2), similar to those of pure $BaTiO_3$. However, T_c of pure $BaTiO_3$ is shifted to a lower temperature and T_1 and T_2 to higher temperatures by the substitution of Zr ion for Ti ion. The anomaly at T_c is relatively sharp and the peak temperature is independent of the measuring frequencies, similar to those observed in pure $BaTiO_3$.

In region II ($0.12 < x < 0.25$) only one rounded anomaly (at T_c) with very small frequency dispersion is found in ε, corresponding to direct transformation from the cubic phase into the rhombohedral one.

In region III ($x > 0.25$) the diffuse maximum of $\varepsilon(T)$ at T_m with obvious frequency dispersion is observed with further increasing Zr content, displaying a typical ferroelectric relaxor behaviour. The results of the three regions show the evolution from a normal ferroelectric to a ferroelectric relaxor with increasing Zr concentration.

In compounds with small Ca doping a wide boundary between zones II and III exists. There is a maximum of $\varepsilon(T)$ at T_m, but in addition a classical ferroelectric phase at $T_3 < T_m$ appears [8, 9].

Heat capacity and thermal expansion studies of the $Ba_{0.92}Ca_{0.08}Ti_{0.76}Zr_{0.24}O_3$ compound reveal three blurred anomalies on the $C_p(T)$ and $\alpha(T)$ dependences at all three specific temperatures characteristic for ferroelectric relaxors: at T_d, where local distortions of cubic phase and polar nanoregions arise; at T_m, the temperature of $\varepsilon(T)$ maximum, and at T_c, where phase transition into the ferroelectric phase with macroscopic polarization takes place [10]. The small value of anomalous heat capacity and the closeness of temperatures T_m, T_d and T_c have not allowed us to separate contributions to ΔC_p and to analyse them within the frames of modern models of relaxors. In $BaTi_{0.65}Zr_{0.35}O_3$ (BTZ35) and $BaTi_{0.60}Zr_{0.40}O_3$ (BTZ40) the difference between T_d and T_m amounts to ∼130–180 K and overlapping of heat capacity anomalies near T_d and T_m are not so strong [7, 11].

The main purpose of the present paper is to clarify the $C_p(T)$ behaviour in the vicinity of T_d and T_m temperatures and to analyse the spherical random bond–random field model (SRBRF) to describe the heat capacity anomaly at T_m.

2. Sample preparation and experimental technique

The $Ba(Ti_{0.65}Zr_{0.35})O_3$ and $BaTi_{0.60}Zr_{0.40}O_3$ compounds were obtained from barium carbonate and from titanium and zirconium oxides:

$$BaCO_3 + (1-x)TiO_2 + xZrO_2 \rightarrow Ba(Ti_{1-x}Zr_x)O_3 + CO_2.$$

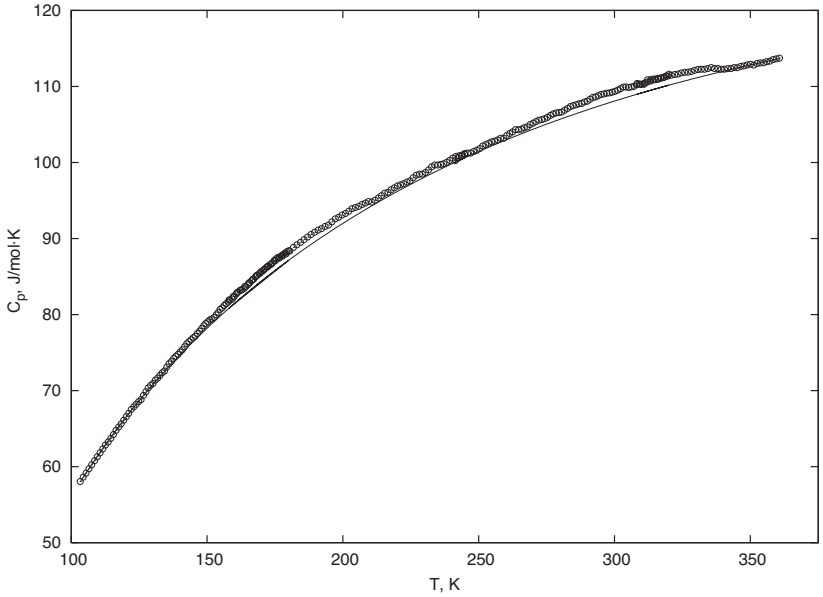

Figure 1. Temperature dependence of the heat capacity of BTZ35. Solid line—lattice heat capacity approximated by the combination of Debye and Einstein functions.

After calcination at temperatures between 1100 and 1300 °C for 15 h under oxygen, disc-shaped ceramic samples with diameter 10 mm and 4–7 mm high were sintered at about 1400 °C for 4 h under an oxygen atmosphere. No sintering additives were used. The grain size was about 1–2 μm, and the density reached 95% of the calculated value. X-ray diffraction analysis confirmed that the samples were single phase and that the compounds had cubic structure $Pm3m$ [2, 3].

Measurements of heat capacity in the temperature range 100–360 K were carried out by the adiabatic calorimeter method, allowing us to obtain the absolute value of integral heat capacity with a high accuracy. The mass of a ceramic sample was 2.7 g for $x = 0.35$ and 3.8 g for $x = 0.40$. Measurements were made using both the traditional method of discrete heating ($\Delta T = 1.0$–2.5 K) and a regime of continuous heating at a temperature variation rate of about $dT/dt \approx (0.1$–$0.3)$ K min^{-1} [12]. The accuracy of measurements depends on the method of heating and amounts to (0.1–0.3)%.

3. Results and discussion

3.1. Heat capacity

The results of heat capacity measurements of BTZ35 ceramic are represented in figure 1. The deviation of experimental points relative to the smoothed curve does not exceed 0.3%. The curve describing the temperature dependence of heat capacity does not exhibit clearly manifested anomalies typical of traditional phase transitions. However, in the temperature regions 250–350 and 150–200 K broad blurred anomalies in $C_p(T)$ are observed. A similar situation is found for BTZ40 ceramic; however, the low-temperature anomaly of heat capacity is displaced a little in the lower-temperature region 120–150 K.

To analyse these features in more detail the anomalous ΔC_p and lattice C_L contributions to the total heat capacity should be separated. This procedure was carried out using a simple

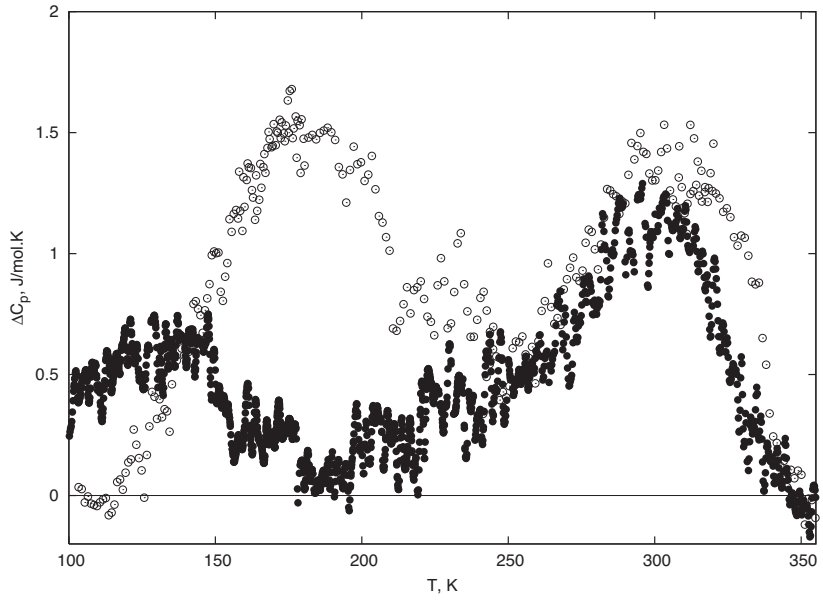

Figure 2. Anomalous heat capacity of BTZ35 (○) and BTZ40 (●).

model describing the lattice heat capacity of the compound by a combination of the Debye and Einstein functions. In the temperature range 100–360 K the heat capacity of samples under investigation is already poorly sensitive to fine details of a vibration spectrum and the approximation of the lattice contribution carried out in the same way is quite justified.

The anomalous component of heat capacity $\Delta C_p = C_p - C_L$ for both compounds under investigation reaches only ∼1.5 J mol^{-1} K^{-1} or ∼1.5% of C_L (figure 2). However, one can see clearly two features in the behaviour of ΔC_p near 310 and 180 K for BTZ35 and near 305 and 135 K for BTZ40.

The entropy change associated with the anomalous behaviour of heat capacity is small ($\Delta S \sim 0.1R$) and demonstrates clearly the displacive nature of crystal phase changes. It should be noted that for barium containing perovskites the heat capacity anomalies and the entropy changes are much smaller [10] than those for lead containing relaxors such as PMN. In the latter, the positional ordering of Pb ions is responsible for the main part of the entropy [13].

Once again we shall note that anomalies of the heat capacity are very small and smeared in a wide temperature range that hinders the determination of the temperature of anomalous contribution appearance. Deviation from regular dependences in $C_p(T)$ is observed below 350 K, where the permittivity curves of both compounds start to deviate from the Curie–Weiss law (the Burns temperature T_d) [7]. The temperatures of the second heat capacity anomaly are close to the temperatures T_m of the permittivity maximum [7].

3.2. Phase diagram of $BaTiO_3$–$BaZrO_3$ system

In order to establish a reason for the heat capacity anomalous behaviour, we will consider the structural features of these materials and the available models describing this phenomena.

Structural study of $BaTi_{1-x}Zr_xO_3$ [14] reveals that the lattice parameter displays a linear evolution with x up to ∼0.25 and obeys the Vegard rule [15] that is characteristic for solid solutions. As this takes place, lattice interactions are changed, and the variation of temperatures

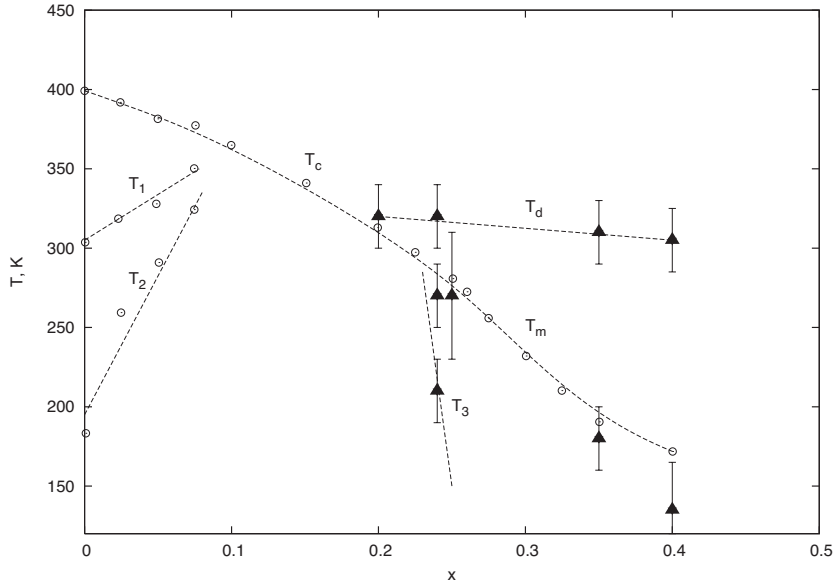

Figure 3. T–x phase diagram of the $BaTi_{1-x}Zr_xO_3$ system. ○—results of dielectric measurements [7], ▲—results of present study and [11].

and sequences of phase transitions is observed (figure 3). A gradual narrowing of intermediate tetragonal and orthorhombic phases and decreasing of transition temperature from the cubic phase are observed.

At zirconium concentration about 20%–30% there is a change of both the temperature and frequency dependences of the permittivity. The anomaly of $\varepsilon(T)$ becomes strongly diffuse, and the T_m value essentially depends on the frequency of the electric field. However, the macroscopic spontaneous polarization below T_m is not observed. Such a behaviour is typical for a relaxor.

This crossover coincides with the appearance of additional reflexes on x-ray patterns as well as the change of concentration dependence of a lattice parameter [14] that apparently indicates a multiphase nature of samples and demixing of solid solutions. Thus, the limit of solid solubility of Zr^{4+} at Ti sites in $BaTiO_3$ is about 0.25. A similar situation was also observed for the $BaTi_{1-x}Ce_xO_3$ [4].

One can suppose that compounds $BaTi_{1-x}Zr_xO_3$ with $x \gtrsim 0.25$ consist of nanoregions with different concentrations of zirconium. Ti^{4+}-rich regions become polar, whereas Zr^{4+}-rich ones remain paraelectric, as well as pure $BaZrO_3$. Thus the long-range order characteristic for the low-temperature phase of barium titanate and solid solutions with $x \lesssim 0.25$ is destroyed at $x \gtrsim 0.25$. The transition temperature of each nanoregion into the polar phase T_{cl} depends on the composition of this nanoregion, and the sample has a certain range of transition temperatures, concentrated near the Burns temperature T_d.

Thus, at $x \gtrsim 0.25$ the situation for $BaTi_{1-x}Zr_xO_3$ compounds is somewhat analogous to one observed earlier for $PbMg_{1/3}Nb_{2/3}O_3$ (PMN), where the compositional inhomogeneity on the nanoscale as well as the presence of polar nanoregions were reliably established [16]. We think that this is the reason why the anomalous heat capacity behaviour is the same for BTZ35, BTZ40 and PMN [13, 17].

3.3. Phase transition in nanoregions and heat capacity anomaly near T_d

The heat capacity anomaly of $BaTi_{1-x}Zr_xO_3$ at T_d is strongly smeared and cannot be described in the frame of thermodynamic theory based on the traditional free energy expansion. Such behaviour of ΔC_p is connected with the distribution of Zr concentrations in nanoregions leading to the distribution of the local transition temperatures. A similar situation was observed in heat capacity study of $BaTiO_3$ polycrystalline thin film [18, 19]. Smearing of the C_p anomaly was considered as a result of the grain size distribution leading to the transition temperature distribution [19].

The heat capacity temperature dependences of $BaTi_{1-x}Zr_xO_3$ we can analyse likewise [19] using minimization of the conventional type of free energy with the coefficients depending on the Zr concentration and taking into account the distribution of the concentration. The free energy view is expressed as

$$F = \frac{A_x}{2}P^2 + \frac{B_x}{4}P^4 + \frac{C_x}{6}P^6, \tag{1}$$

where

$$A_x \approx \alpha \cdot (T - T_{\mathrm{cl}}(x)), \qquad B_x \approx b, \qquad C_x \approx c, \tag{2}$$

T_{cl} is the local phase transition temperature of nanoregion and b and c are constants.

Let us suppose that the distribution function of concentration has a Gaussian form:

$$f(x) = C \cdot \exp\left[-\left(\frac{x - x_0}{\sigma_x}\right)^2\right]. \tag{3}$$

One can see (figure 5) that the phase transition temperature dependence on Zr concentration is approximately linear in the vicinity of $x \approx 0.2$–0.25. In this case the distribution function of T_{cl} has a Gaussian form too

$$F(T, T_{\mathrm{cl}}^0, \sigma_T) = f(x) \cdot \frac{\mathrm{d}x}{\mathrm{d}T_{\mathrm{cl}}} = C_T \cdot \exp\left[-\left(\frac{T - T_{\mathrm{cl}}^0}{\sigma_T}\right)^2\right], \tag{4}$$

with normalization constant

$$C_T = \frac{2}{\sigma_T\sqrt{\pi}\left[\mathrm{erf}\left(\frac{T_{\mathrm{cl}}^0}{\sigma_T}\right) + 1\right]}. \tag{5}$$

To obtain the temperature dependence of the heat capacity observed, we have performed the averaging of the equation

$$\Delta C_p = \frac{\alpha^2}{2b}\frac{T}{\sqrt{1 + \frac{4\alpha c}{b^2}(T_{\mathrm{cl}}(x) - T)}} \qquad T < T_{\mathrm{cl}} \tag{6}$$

with the help of the distribution function $F(T, T_{\mathrm{cl}}^0, \sigma_T)$ in the form given by equation (4):

$$\Delta C_p(T_{\mathrm{cl}}^0, T, \sigma_T) = \frac{\alpha^2 T}{2b}\int_0^{T_{\mathrm{c}}} \frac{F(T_{\mathrm{cl}}, T_{\mathrm{cl}}^0, \sigma_T)\,\mathrm{d}T_{\mathrm{cl}}}{\sqrt{1 + \frac{4\alpha c}{b^2}(T_{\mathrm{cl}} - T)}}. \tag{7}$$

The results of the experimental data approximation on the basis of equation (7) in the vicinity of T_{d} are presented in figure 4 (BTZ35: $T_{\mathrm{cl}}^0 = 318$ K, $\sigma_T = 25$ K) and figure 5 (BTZ40: $T_{\mathrm{cl}}^0 = 313$ K, $\sigma_T = 22$ K) by chain lines. The most probable transition temperatures T_{cl}^0 and σ_T values are rather close for both samples and correspond to the most probable concentration of polar nanoregions $x_0 \approx 0.20$ with $\sigma_x \approx 0.05$.

The data obtained allow us to separate and analyse the anomalous part of heat capacity connected with processes taking place near T_{m}.

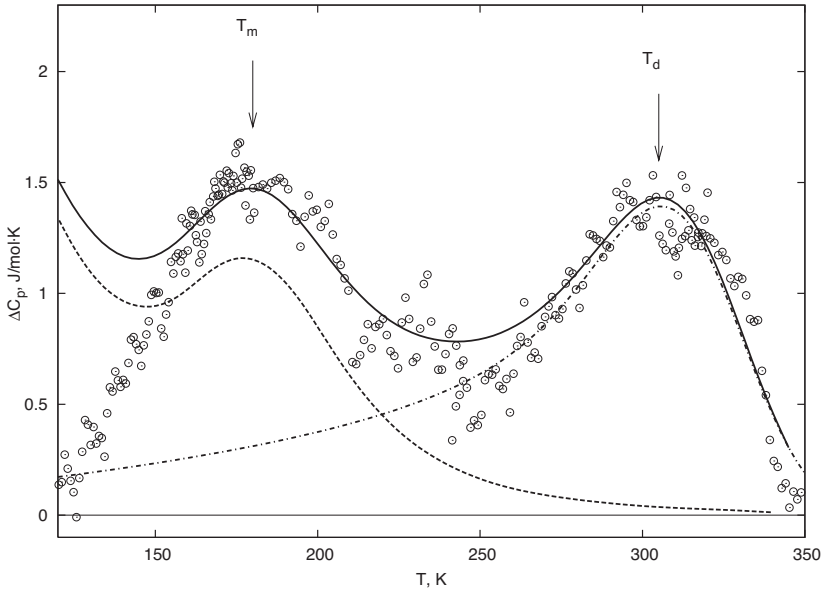

Figure 4. Anomalous heat capacity of BTZ35.

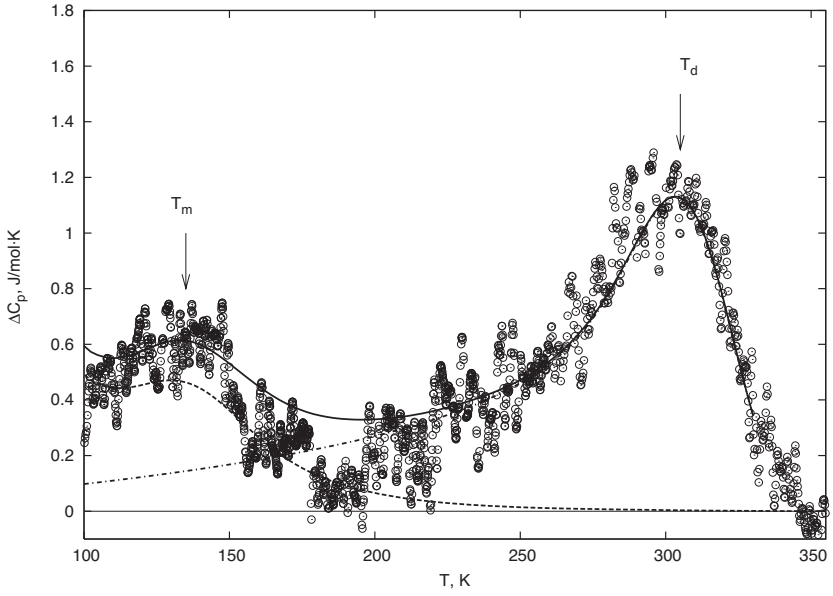

Figure 5. Anomalous heat capacity of BTZ40.

3.4. SRBRF model and heat capacity anomaly at T_m

To describe the behaviour of relaxors containing interacting polar nanoregions at temperatures $T < T_d$, a spherical random bond–random field model (SRBRF) was proposed [20]. In spite of its simplicity, this model captures a number of physical features of relaxors considering a system of coupled, randomly reorienting polar nanoclusters in the presence of random electric

fields. It is assumed that both random interactions (or bonds) and random electric fields have Gaussian distributions and the model Hamiltonian has the following form [20]:

$$H = -\frac{1}{2}\sum J_{ij}\vec{S}_i\vec{S}_j - \sum \vec{h}_i\vec{S}_i - g\vec{E}\sum \vec{S}_i, \tag{8}$$

where $\vec{S}_i$ is the dipole moment of the ith polar cluster, J_{ij} the random intercluster interactions (J_0—mean value, J^2—variance), $\vec{E}$ the external electric field and $\vec{h}_i$ the random local electric fields ($\langle h\rangle = 0$—mean value, $\langle h^2\rangle \equiv \Delta \neq 0$—variance). For $J_0 < \sqrt{J^2+\Delta}$ long-range order cannot exist and the system is in a spherical glass (SG) phase at all temperatures with a nonzero value of the order parameter $q \sim \sum_i \langle S_i\rangle^2$. If $\Delta = 0$ as in magnetic spin glasses, a transition from a high-temperature paraelectric to SG phase occurs at $T_m = J/k$. For $\Delta \neq 0$ and $\Delta \ll J^2$ the sharp transition disappears, but the nonlinear susceptibility shows a maximum at $T_m \approx (\sqrt{J^2+\Delta})/k$. For $J_0 > \sqrt{J^2+\Delta}$ long-range order ($P \sim \sum_i \langle S_i\rangle \neq 0$) is possible and a phase transition to an inhomogeneous ferroelectric phase occurs below the critical temperature

$$T_c = \frac{J_0}{k}\left(1 - \frac{\Delta}{J_0^2 - J^2}\right). \tag{9}$$

In the case of BTZ35 and BTZ40 the interaction parameter J_0 is apparently smaller than the critical value, and a transition to the ferroelectric phase with a macroscopic order parameter (polarization) is not observed and classical heat capacity anomalies are also absent. However, the existence of nonzero parameter q as well as its temperature variation lead to an additional contribution to free energy and hence to heat capacity.

The equilibrium values of the polarization P and the order parameter q can be determined from the saddle-point conditions of the free energy [20]

$$-\tfrac{2}{3}\beta f = \beta J_0 P^2 - \tfrac{1}{2}\beta^2 J^2 q^2 - 2z + \ln(2z + \beta^2 J^2 q) - \frac{\beta^2}{2}\frac{J^2 q + \Delta + (J_0 P + gE)^2}{2z + \beta^2 J^2 q}, \tag{10}$$

where z is a Lagrange multiplier introduced to enforce the spherical conditions [20]:

$$\begin{aligned} P &= \beta(1-q)(J_0 P + gE), \\ q &= \beta^2(1-q)^2(J^2 q + \Delta) + P^2, \\ 2z &+ \beta^2 J^2 q = 1/(1-q). \end{aligned} \tag{11}$$

Using the free energy expression (10) and the solution of system (11) for the relaxor state ($P = 0$, $q \neq 0$) we can obtain the temperature dependence of heat capacity $\Delta C_p(T)$ and evaluate parameters J and Δ of the model from the experimental data fitting. The results are represented in figures 4 and 5 by a dashed line. The total anomalous heat capacity is shown by a solid line. One can see that these lines give a comparatively good fit of the experimental points except the temperature region $T < T_m$. We suppose that this deviation is connected with the Lagrange multiplier z temperature dependence which is enhanced with increase of random field variance Δ. The SRBRF model as a classical continuous model gives a negative value of the entropy in the low temperature limit and its predictions become incorrect at $T \to 0$. For BTZ35 and BTZ40 the best possible fit was obtained at $J/k_B = 180$ K, $\Delta/J^2 = 0.020$ and $J/k_B = 135$ K, $\Delta/J^2 = 0.033$ accordingly.

We have performed a similar analysis for the relaxor $PbMg_{1/3}Nb_{2/3}O_3$ using the experimental data obtained earlier [13]. In figure 6 one can see that the anomalous heat capacity of PMN near T_m can be described in the frame of the SRBRF model with $\Delta/J^2 = 0.045$. This value is very close to $\Delta/J^2 = 0.05$ evaluated from the ^{207}Pb NMR line shape [21].

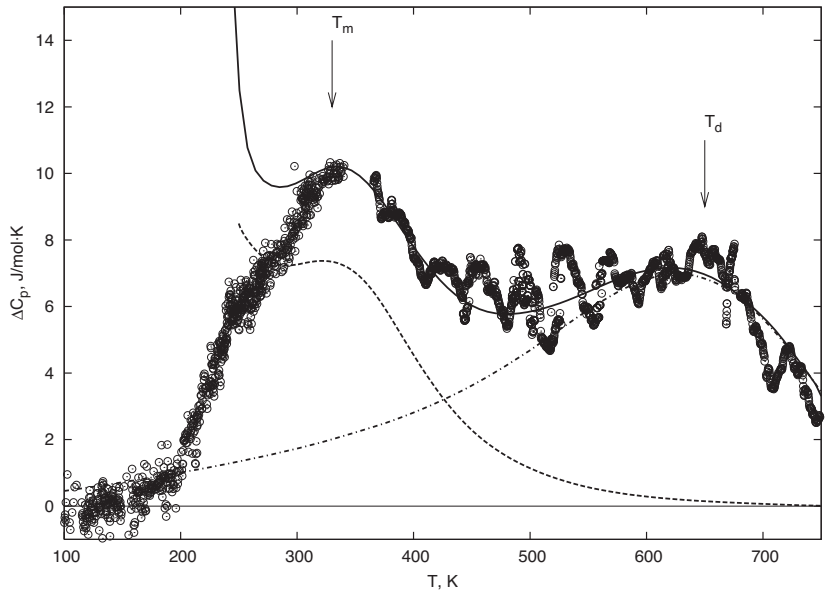

Figure 6. Anomalous heat capacity of $PbMg_{1/3}Nb_{2/3}O_3$.

4. Conclusions

Precise specific heat measurements have been performed over a wide temperature range between 100 and 360 K for $BaTi_{1-x}Zr_xO_3$ relaxors. Heat capacity anomalies related to the polar region formation near the Burns temperature T_d and to the maximum of the permittivity at T_m have been found. The value of entropy change at T_d is rather small and thus the mechanism of polar nanoregion formation can be considered as displacive. The anomalous heat capacity near T_m can be described by the SRBRF model. The value of the random field variance for $BaTi_{1-x}Zr_xO_3$ compounds is half that for PMN.

Acknowledgments

This work was supported in part by the KRSF-RFBR (grant no 05-02-97707-r-enisey-a) and a grant from the President of the Russian Federation for support of leading scientific schools (NSh-4137.2006.2). One of the authors (VB) would like to thank the Lavrentev's competition for Young Scientists of SB RAS (grant N 51).

References

[1] Hennings D, Schnell A and Simon G 1982 *J. Am. Ceram. Soc.* **65** 539
[2] Ravez J and Simon A 1997 *Eur. J. Solid State Inorg. Chem.* **34** 1199
[3] Farhi R, Marssi M El, Simon A and Ravez J 1999 *Eur. Phys. J.* B **9** 599
[4] Ang C, Jing Z and Yu Z 2003 *J. Mater. Sci.* **38** 1057
[5] Ravez J and Simon A 2000 *Phys. Status Solidi* a **178** 793
[6] Samara G A 2003 *J. Phys.: Condens. Matter* **15** R367
[7] Simon A, Ravez J and Maglione M 2004 *J. Phys.: Condens. Matter* **16** 963
[8] Ravez J, van der Mühll R, Simon A and Sciau Ph 1999 *J. Mater. Chem.* **9** 2829
[9] Sciau Ph and Castagnos A M 2002 *Ferroelectrics* **270** 259

[10] Gorev M V, Flerov I N, Bondarev V S, Sciau Ph and Savariault J-M 2004 *J. Phys.: Condens. Matter* **16** 7143
[11] Gorev M V, Bondarev V S, Flerov I N, Sciau Ph and Savariault J-M 2005 *Sov. Phys.—Solid State* **47** 2212
[12] Gorev M V, Gekk P I, Iskornev I M, Kot L A, Gonyaev V S, Flerov I N and Cherepanov V A 1988 *Izmer. Tekh.* **8** 33
[13] Gorev M V, Flerov I N, Bondarev V S and Sciau Ph 2003 *JETP* **96** 531
[14] Pantou R, Dubourdieu C, Weiss F, Kreisel J, Kobernik G and Haessler W 2003 *Mater. Sci. Semicond. Process.* **5** 237
[15] Vegard L 1921 *Z. Phys.* **5** 17
[16] Miao S, Zhu J, Zhang X and Cheng Z-Y 2001 *Phys. Rev.* B **65** 0522101
[17] Moriya Y, Kawaji H, Tojo T and Atake T 2003 *Phys. Rev. Lett.* **90** 205901
[18] Strukov B A, Davitadze S T, Kravchun S N, Taraskin S A, Goltzman M, Lemanov V V and Shulman S G 2003 *J. Phys.: Condens. Matter* **15** 4331
[19] Glinchuk M D and Bykov P I 2004 *J. Phys.: Condens. Matter* **16** 6779
[20] Pirc R and Blinc R 1999 *Phys. Rev.* B **60** 13470
[21] Blinc R, Gregorovic A, Zalar B, Pirc R, Laguta V V and Glinchuk M D 2001 *Phys. Rev.* B **63** 024104